J. Phys. Chem. A **2004,** *108,* 7895−7902

Tunable Synchrotron Vacuum Ultraviolet Ionization, Time-of-Flight Investigation of the Photodissociation of *trans*-Crotonaldehyde at 193 nm[†]

Jinian Shu,[‡] Darcy S. Peterka,[‡,§] Stephen R. Leone,[‡,§] and Musahid Ahmed*,[‡]

Departments of Chemistry and Physics, University of California, and Lawrence Berkeley National Laboratory, Berkeley, California 94720

Received: January 26, 2004; In Final Form: May 28, 2004

Photodissociation of the unsaturated *trans*-crotonaldehyde ($CH_3CHCHCHO$) molecule at 193 nm is studied using photofragment translational spectroscopy (PTS) and detected by ionization with tunable synchrotron ultraviolet radiation. The photofragment time-of-flight (TOF) spectra at $m/e = 68(C_4H_4O^+)$, $55(C_3H_3O^+)$, $41(C_3H_5^+)$, $40(C_3H_4^+)$, $39(C_3H_3^+)$, 29(?), $28(CO^+)$, $27(C_2H_3^+)$, $26(C_2H_2^+)$, and $15(CH_3^+)$ are measured. Mass 29 could not be unambiguously assigned. Analysis of these experimental results reveals three dissociation channels: $H + C_4H_5O$, $CH_3 + C_3H_3O$, and $CO + C_3H_6$. A fourth channel associated with mass 29 could reflect either formation of HCO or C_2H_5. The measurements also indicate that C_3H_6 undergoes strong secondary dissociation. The center of mass (CM) translational energy distributions obtained by fitting the TOF mass spectra of the fragments yield values 42, 23, and 43 kJ/mol average CM kinetic energies for the $H + C_4H_5O$, $CH_3 + C_3H_3O$ and $CO + C_3H_6$ channels, respectively. The photoionization yield curve of the CHCHCHO radical is measured for the first time with an onset ≤7.6 eV. The photodissociation mechanism of crotonaldehyde is compared with the photodissociation dynamics of acrolein (CH_2CHCHO).

I. Introduction

Carbonyl compounds are ubiquitous in the atmosphere. They are often of significance as precursors of radicals. Crotonaldehyde, a small unsaturated carbonyl compound, is emitted in the troposphere from biogenic sources and the partial oxidation of fuels. It may also arise as a secondary pollutant from atmospheric oxidation of volatile organic compounds.[1−3] Crotonaldehyde is removed from the atmosphere by photolysis or reaction with oxidizers such as OH, O_3, and NO_3.

Numerous investigations have been conducted on the vapor-phase photolysis of crotonaldehyde.[4−18] The UV−visible absorption spectrum of crotonaldehyde has two absorption bands. The first absorption band extends from 190 to 250 nm, with a maximum at around 203 nm, and it is assigned to the $S_2 \leftarrow S_0$ transition.[15,18] The second band is located between 250 and 400 nm and is slightly structured at wavelengths greater than 360 nm. It is assigned to the $S_1 \leftarrow S_0$ transition. In early studies on the vapor-phase photochemistry of *trans*-crotonaldehyde, the photodecomposition products CO, propylene, C_2H_4, H_2, CH_4, allene, propyne, and cyclopropane were reported when irradiated with photons in the 238−400 nm range.[16,17] The major photodecomposition products were CO and propylene.[16,17] Other studies showed that photoisomerization led to the formation of 3-butene-1-al, ethylketene, and enol-crotonaldehyde.[7,17] Recently, Magneron et al. reported the 275−380 nm photolysis of crotonaldehyde in the presence of radical scavengers.[18] However, no radical products of crotonaldehyde photolysis were observed under their experimental conditions. Two very recent studies have focused on the photodissociation of crotonaldehyde.[19,20] At the CCSD(T)/6-311G//B3LYP/6-311++G level of theory, the Chen group calculated the dissociation and isomerization of the crotonaldehyde molecule through its S_0, T_1, T_2, and S_1 states.[19] Their calculations show that isomerization is a very important process in the photodissociation of crotonaldehyde. The study done by Stolow and co-workers shows that the absolute absorption cross-section for ground state HCO formation from crotonaldehyde is less than 0.35% of that of acrolein in the photodissociation studies at 193 nm.[20] They postulate that the methyl group on the crotonaldehyde molecule hinders the $S_1 \rightarrow T_2$ intersystem crossing greatly and that it is dissociation from the T_2 state that would lead to ground-state HCO.

An analogue of crotonaldehyde, acrolein (CH_2CHCHO) is the smallest unsaturated carbonyl compound and its photodissociation dynamics can serve as an aid in understanding crotonaldehyde photodissociation. The structural difference between the two molecules is that crotonaldehyde has a CH_3 group on its γ carbon atom, whereas acrolein has a hydrogen atom. Compared with crotonaldehyde, acrolein has attracted more attention, and more extensive studies on its photodissociation have been performed.[21−38] The UV−visible absorption spectra of acrolein is similar to that of crotonaldehyde but is shifted about 5−10 nm to the blue.[15] In the acrolein photodissociation, three primary channels, the CO, HCO, and H loss channels, have been observed in the near UV to UV range.[22−31] In vapor-phase photochemistry studies, the major photoproducts observed in the near UV range photolysis and in the Hg($^3P_1$)-sensitized decomposition of acrolein were CO and C_2H_4.[6,22,23] Recently, photodissociation experiments under collision-less conditions clearly revealed the three primary dissociation channels mentioned above for the acrolein photodissociation.[25−38] Many theoretical calculations of the photodissociation of acrolein have been carried out.[32−37] The recent theoretical work of Fang presents a picture for the mechanisms of the three

---

[†] Part of the special issue “Richard Bersohn Memorial Issue”.

* Corresponding author. Phone: (510)486-6355. Fax: (510)486-5311. E-mail:mahmed@lbl.gov.

[‡] Lawrence Berkeley National Laboratory.

[§] UC Berkeley.

10.1021/jp049638d CCC: $27.50

primary dissociation channels of acrolein.[37] The mechanisms suggested by Fang were inferred from the configuration and potential energy profiles of the S_0, S_1, and T_1 electronic states and can be simply expressed as the following processes:

$$\text{(a) } C_3H_4O(S_2) \xrightarrow{R} C_3H_4O(T_1) \xrightarrow{\text{ISO}} CH_3CHCO \rightarrow CH_3CH + CO \xrightarrow{\text{ISO}} C_2H_4 + CO$$

$$\text{(b) } C_3H_4O(S_1) \xrightarrow{\text{ISC}} C_3H_4O(T_1) \rightarrow CH_2CH + CHO$$

$$\text{(c) } C_3H_4O(S_2) \xrightarrow{R} C_3H_4O(S_1) \xrightarrow{\text{IC}} C_3H_4O(S_0) \rightarrow CH_2CHCO + H$$

where the R, ISO, ISC, and IC stand for relaxation, isomerization, intersystem crossing, and internal conversion, respectively.

Here we briefly note the differences in the photodissociation of the saturated aldehydes compared with unsaturated aldehydes. The UV absorption of small saturated aldehydes is similar to the near UV absorption of acrolein and crotonaldehyde, which results in pumping of one lone pair electron from the σ orbital of the oxygen atom to the antibonding π orbital of the C=O bond. This transition is labeled as the $S_1 \leftarrow S_0$ transition.[39] In studies of the photodissociation of the small saturated aldehydes, two major dissociation channels have been observed and discussed.[39−41]

$$\text{(d) } RCHO \rightarrow RH + CO$$

$$\text{(e) } \qquad\quad \rightarrow R + HCO$$

Here R stands for H, CH_3, and CH_3CH_2 in the case of formaldehyde, acetaldehyde, and propanal, respectively. The mechanisms for the photodissociation of these saturated aldehydes are believed to be that the radical (HCO) loss channel proceeds along the T_1 potential surface via a $S_1 \rightarrow T_1$ intersystem crossing whereas the molecular (CO) loss channel proceeds along the S_0 potential surface via a $S_1 \rightarrow S_0$ internal conversion.[41]

In this work, the 193 nm photodissociation of crotonaldehyde has been studied by using photofragment translational spectroscopy with tunable synchrotron radiation as the photoionization source. Analysis of the experimental results reveals that the dissociation of crotonaldehyde at 193 nm yields three channels: $CH_3CHCHCO + H$, $CH_3 + CHCHCHO$, and $CO + CH_3CHCH_2$. A fourth channel associated with mass 29 could reflect formation of either HCO or C_2H_5. The observed channels are very similar to those of the photodissociation of acrolein excited at 193 nm.

II. Experimental Section

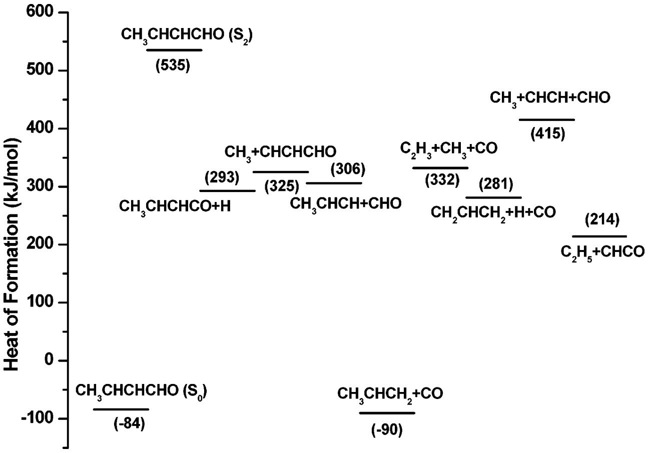

Figure 1. Energy diagram for possible reaction channels of photodissociation of crotonaldehyde at 193 nm excitation. The standard enthalpies (298 K) of $CH_3CHCHCHO^*$, H, $CH_3CHCHCO^*$, CH_3, $CHCHCHO^*$, HCO, CH_3CHCH^*, CO, CH_3CHCH_2, CH_2CHCH_2, C_2H_3, CH_3CCH, C_2H_2, C_2H_5, and $CHCO^*$ are −84, 218, 75, 145, 180, 43, 263, −110, 20, 171, 297, 185, 227, 119, and 95 kJ/mol, respectively (* are estimated values). The relative heats of formation and bond energies used for calculating these heats of formation are obtained by referring to *65th CRC Handbook of Chemistry and Physics* and *webbook.nist.org*.

Photofragment translational spectra for crotonaldehyde at 193.3 nm are obtained using a previously described crossed molecular beam apparatus.[42] This machine consists of a rotatable chamber source for the molecular beam, a main chamber, and a detector chamber. The detector consists of a port for synchrotron vacuum ultraviolet light ionization, a quadrupole mass filter (Extrel), and a Daly particle detector. The synchrotron light is generated by a 10 cm period undulator on Beamline 9.0.2 at the Advanced Light Source at Berkeley. The transient signal output from the Daly detector is discriminated and collected by a multichannel scalar (EG&G Ortec, Turbo-MCS). A Lambda Physik LPX210i excimer is used to generate up to 50 mJ/pulse of light at a 100 Hz repetition rate for the photolysis. The unpolarized laser light is loosely focused into the main chamber with a $f \approx 50$ cm lens, forming a 2.5×6 mm laser spot at the interaction region. In this experiment, the energy of the laser beam is attenuated with stainless steel meshes to achieve the final desired energy. Almost all of the time-of-flight (TOF) spectra in this paper are collected with 1−3 mJ/pulse of laser energy. Great care is taken to ensure that the TOF data are free of multiphoton effects. The bandwidth of synchrotron light is about 3%. The synchrotron light emitted from the undulator passes through a gas filter filled with argon to remove higher order harmonic radiation from the undulator. A 1 mm thick MgF_2 window positioned in the beam path of the synchrotron light removes any remaining high energy radiation; however, this can only be used for light with energy lower than 10.6 eV. The *trans*-crotonaldehyde (99.9%) sample is supplied by Aldrich and helium (99.999%) is obtained from Spectra Gases. The compound is used without further purification. An 800 Torr (1.06×10^5 Pa) mixture consisting of about 4% crotonaldehyde in helium is prepared by bubbling helium through the room-temperature crotonaldehyde. The mixture is fed through a pulsed valve heated to 115 °C to reduce the formation of clusters. The resulting molecular beam enters the main chamber and intersects the laser beam after being collimated with a 1.5 mm diameter orifice skimmer. The speed of the molecular beam is measured both by chopping the beam and by laser depletion hole-burning methods. The results of these two methods agree with each other very well. The speed of the crotonaldehyde beam is about 1560 m/s with a speed ratio of about 11 and an angular divergence of about ±1°. A forward convolution program is used to analyze the laboratory TOF spectra. The program takes into account the spread of beam velocity, the length of the laser spot, the angular divergence of the molecular beam, and the collection angle of the detector.

III. Results

The available energies of reaction for the possible photodissociation channels of crotonaldehyde excited at 193.3 nm (618.9 kJ/mol) are shown in Figure 1. In this experiment, signals at $m/e = 68$, 55, 41, 40, 39, 29, 28, 27, 26, and 15 are observed. They correspond to $C_4H_4O^+$, $C_3H_3O^+$, $C_3H_5^+$, $C_3H_4^+$, $C_3H_3^+$,

HCO^+ or $C_2H_5^+$, CO^+, $C_2H_3^+$, $C_2H_2^+$, and CH_3^+ respectively. We ensure that these signals result from single 193 nm photon photodissociation by checking the laser power dependence of signals. With the help of the information obtained from the TOF spectra at these masses, we derive three primary dissociation channels for photodissociation of crotonaldehyde at 193.3 nm. These are the $H + CH_3CHCHCO$, $CH_3 + CHCHCHO$, and $CO + C_3H_6$ channels, discussed next. The fourth dissociation channel, which leads to formation of mass 29, could come from either HCO or C_2H_5 and is discussed later.

A. $H + CH_3CHCHCO$ Dissociation Channel. Among the ions observed in this experiment, the $m/e = 68$ $C_4H_4O^+$ is the heaviest. We could not detect any dissociation signal at mass 69, which could occur at small laboratory angles, because of the large background ions resulting from dissociative photoionization of the crotonaldehyde beam. We assign the signal at mass 68 to the single H loss channel of crotonaldehyde photodissociation because of the following considerations. We first exclude the possibility of diradical formation by loss of two H atoms in a single step in this experiment because the energy of a single 193.3 nm photon (618.9 kJ/mol) is not enough to cause the crotonaldehyde molecule to break two C−H bonds simultaneously. Second, we exclude direct H_2 formation as a contributor to the signal at mass 68 because the observed mass carries little kinetic energy (if the data of mass 68 were fitted as the products of a H_2 loss channel, the maximum CM kinetic energy would be 109 kJ/mol). As H_2 formation would result from two C−H bond cleavages together with formation of one C−C bond and one H−H bond, the available energy, and thus the energy deposited into translational motion is expected to be greater than the 109 kJ/mol that we would measure for the H_2 loss dissociation. Additionally, the expected barrier to H_2 formation along the pathway for dissociation should make the products have even more kinetic energy when compared with a single C−H bond cleavage, which occurs without a barrier. We believe that the $C_4H_4O^+$ mass is an indication of the H loss from C_4H_5O. Mass 68 ($C_4H_4O^+$) may be formed through one or both of the two different processes shown below:

(f) $C_4H_6O + h\nu_{193nm} \rightarrow C_4H_5O + H$

$\hookrightarrow C_4H_5O + h\nu_{VUV} \longrightarrow C_4H_4O^+ + H$

(g) $C_4H_6O + h\nu_{193nm} \rightarrow C_4H_5O + H$

$\hookrightarrow C_4H_4O + H$

$\quad \xrightarrow{h\nu_{VUV}} C_4H_4O^+ + H$

We believe that process f is more likely for the $C_4H_4O^+$ formation. Process g is only possible for the highly internally excited C_4H_5O fragments, which may lose one more H by breaking a C−H bond and forming one C−C bond. The products from these two different processes may have slightly different kinetic energy distributions. However, we cannot discriminate them in this experiment because the heavy fragment carries only little of the total kinetic energy from dissociation. Direct H atom measurement may be a good way to resolve the H loss channel information. Unfortunately, the signal at mass 1 is too weak for us to obtain a TOF spectrum. To simplify this problem, we treat the signal at mass 68 as the direct product of the H loss channel (mass 69). Under this assumption, the TOF spectra of mass 68 are thought to directly reflect the kinetic energy distribution of C_4H_5O, the product of the H loss channel. It should be noted that this simplification could distort the real kinetic distribution of the H loss channel. However, because the available energy in secondary dissociation (0−99 kJ/mol, estimated) is much less than that in primary dissociations (242 kJ/mol), we think that this simplification is reasonable for secondary dissociation. The amount of the translational energy pumped into daughter ions during the dissociative photoionization process is hard to estimate. But the shape of the TOF spectra of the daughter ion is usually very similar to its parent ion when the energy of the VUV photon is just slightly higher (0.5 eV) than the ion appearance potential. Furthermore, the flight time from the ionization region compared to the photodissociation region to the ion detector is much shorter (less than half). This, we believe, leads to lesser distortion in the kinetic energy curves in the case of dissociative photoionization compared to secondary dissociation.

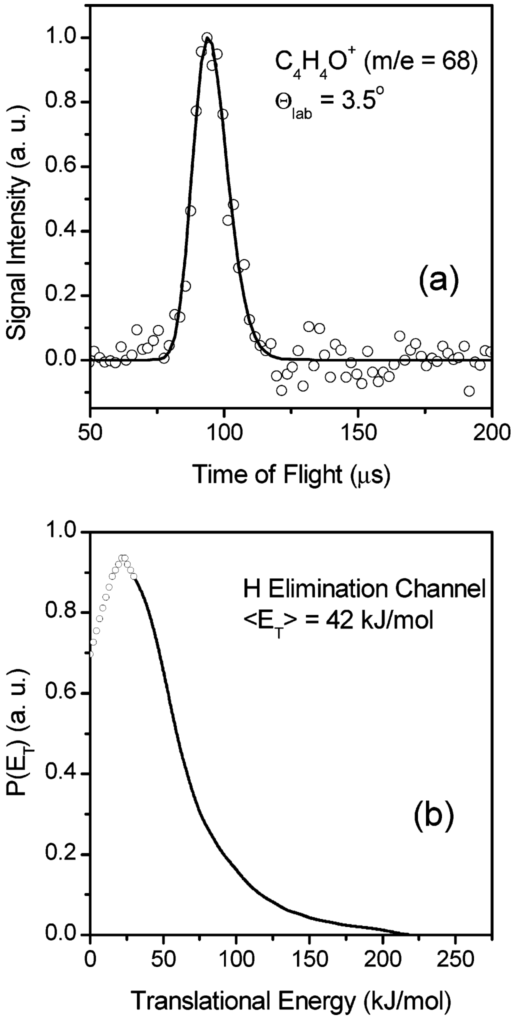

Figure 2. (a) TOF spectra of mass 68 ($C_4H_4O^+$) detected at 3.5° laboratory angle with 10.6 eV photons. TOF spectra of all masses observed in this experiment are collected over a number of laboratory angles; the range being 10−30° for light fragments and 3.5−15° for heavy fragments. Only one-angle TOF spectra of each mass are shown in this paper to save space. The open circles stand for the experimental data points, whereas the solid curve represents the fit to the data in all plots in this paper. (b) The CM translational energy distribution of the H elimination channel. The solid curve is directly derived from the TOF spectra of mass 68. The dots are an extrapolation based on the H loss channel of 193 nm photodissociation of acrolein.

The TOF spectrum at mass 68 measured at a laboratory angle of 3.5° is shown in Figure 2a. Because of the kinetic energy partitioning between the photofragments, the fragment at mass 69 is limited to a very small lab angle. Fragments at mass 69 with kinetic energy lower than 25 kJ/mol in the center-of-mass frame are very difficult to measure, because those fragments overlap with the parent crotonaldehyde beam. Changing the carrier gas to neon from helium to slow the velocity of the molecular beam did not alleviate the problem. The translational energy distribution $P(E_T)$ (the solid curve shown in Figure 2b) for the $C_4H_5O + H$ channel is directly obtained by fitting the TOF spectra of mass 68. The dotted points shown in Figure 2b are a part of the possible $P(E_T)$ for the H elimination channel made by an extrapolation based on the H elimination channel of acrolein.[27] The CM cutoff translational energy of the H loss channel is ≈217 kJ/mol (see Figure 2b). The average CM kinetic energy of this channel is about 42 kJ/mol. The secondary dissociation of fragments usually occurs in those fragments that have small amounts of the available energy in translation (in other words, more energy in internal degrees of freedom), which results in an apparent truncation in the low energy part of the $P(E_T)$ curve. We did not find an obvious truncation in this $P(E_T)$, which usually would indicate a strong secondary dissociation of the nascent hot fragment without absorbing a second photolysis photon. That implies that C_4H_5O does not have any significant secondary dissociation channels other than H atom loss. In acrolein, a theoretical study assigned the hydrogen atom that is lost in the primary dissociation to be the aldehyde hydrogen atom.[37] This may also apply to the photodissociation of crotonaldehyde because the aldehydic C−H bond is the weakest C−H bond in the crotonaldehyde molecule.

B. CH_3 + CHCHCHO Dissociation Channel. Mass 55 is assigned to the photoionization of the C_3H_3O radical, the product of the CH_3 + CHCHCHO dissociation channel. The signal at mass 55 is collected using 8.8 eV synchrotron light. The TOF spectrum of mass = 55 ($C_3H_3O^+$) measured at a 10° laboratory angle is shown in Figure 3a. The translational energy distribution $P(E_T)$ is shown in Figure 3b. The maximum translational energy is ≈113 kJ/mol with an average CM kinetic energy of ≈23 kJ/mol. Similarly to the H loss channel, the $P(E)$ curve generated from the mass 55 TOF also did not show evidence of any strong secondary dissociation. The counter-fragment of CHCHCHO is mass 15. However, the observed total TOF spectra of mass 15 could not be fit with the $P(E_T)$ derived from the TOF spectra of mass 55. We believe this is due to the TOF spectra of mass 15 being badly contaminated by the secondary dissociation of C_3H_6, the product of the CO loss channel (discussed later).

The photoionization yield spectrum of the CHCHCHO radical (shown in Figure 3c) is measured at a laboratory angle of 10° by varying the photoionization photon energy. The points are experimental data, and the curve is a spline fit. The experimental data are normalized by the VUV power. The drop in ion yield at higher energy could be due to dissociative photoionization that would lead to the decrease in signal at mass 55. An upper limit of the ionization onset of 7.6 eV is obtained. Lower photon energies could not be reached with the storage ring running in a 1.9 GeV operation.

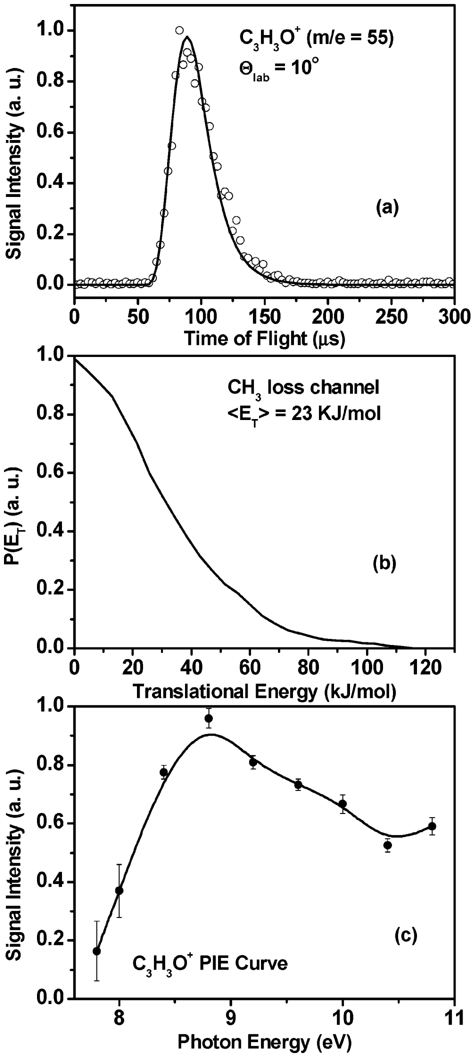

Figure 3. (a) TOF spectra of mass 55 ($C_3H_3O^+$) detected at 10° laboratory angle using 8.8 eV photons. (b) CM translational energy distribution of the CH_3 elimination channel. (c) Photoionization efficiency curve of $C_3H_3O^+$ (m/e = 55).

C. Mass 29 (HCO/C_2H_5) Dissociation Channel. The signal at mass 29 is observed in this experiment. (Figure 4a). The translational energy distribution $P(E_T)$ derived from this TOF is shown in Figure 4b. The average energy released into this channel is 24 kJ/mol and the energy tails out to about 130 kJ/mol. The intensity of the signal at mass 29 is about 20% of that of mass 28 (CO^+). There are only two possible contributors to mass 29, HCO and C_2H_5. Unfortunately, we cannot distinguish these two radicals because their ionization energies are nearly identical (8.12 eV (HCO) vs 8.117 eV (C_2H_5)). Their respective counterfragments cannot be distinguished easily either because no literature ionization energies have been reported. We initially assigned mass 29 to HCO^+ and performed an elaborate analysis assuming mass 29 was the formyl radical, consistent with the photodissociation of acrolein, in which copious amounts of HCO have been observed. However, in light of very recent results, where almost no HCO was observed following the photodissociation of crotonaldehyde,[20] it is possible that C_2H_5 may be the fragment that we observe at mass 29. CHCHCHO, the CH_3 loss channel product, could also contribute to the signal at mass 29 after dissociative photoionization or secondary dissociation. By comparing the shapes of the TOF spectra of mass 29 at 9.3, 10.3, and 12.8 eV (not shown) we rule out any apparent contribution to the signal at mass 29 from dissociative photoionization of the CHCHCHO. Furthermore, we do not find any evidence of secondary dissociation in the $P(E_T)$ of the CH_3 channel derived from the TOF mass spectra of mass 55 ($CHCHCHO^+$). A small contribution from the counterpart of mass 29 ($CHCO^+$ or CH_3CHCH^+) is found in the TOF spectra of mass 41 obtained with <9.3 eV photons. This contribution dissappears when the VUV photon energy is higher than 9.3 eV. However, we find that the TOF mass spectra of mass 40 can be fit very well with the $P(E_T)$ obtained from mass 29. As the signal at mass 40 only appears when the VUV photon energy is higher than 9.3 eV, we suggest that this arises from the dissociative photoionization of CHCO or CH_3CHCH.

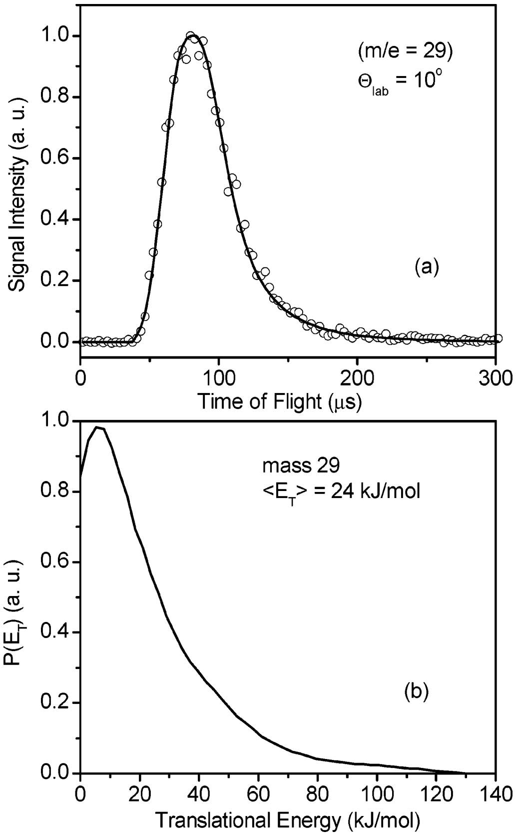

Figure 4. (a) TOF spectra of mass 29 (HCO^+) detected at 10° laboratory angle using 9.3 eV photons. (b) CM translational energy distribution of the HCO elimination channel.

D. CO + C_3H_6 Dissociation Channel. CO and C_3H_6 are the two primary products in the CO loss channel of crotonaldehyde. The mass-to-charge ratios of CO^+ and $C_3H_6^+$ are 28 and 42, respectively. In this experiment, signals directly related to the CO loss channel are observed at mass 28, 39, and 41. No signal at mass 42 is observed. The reason we assign the signals at masses 39 and 41 to the CO loss channel is that the time-of-flight mass spectra of mass 39 and 41 do not match the $P(E_T)$ obtained from the mass 29 loss channel; however, those from masses 39 and 41 can be fit with the $P(E_T)$ obtained from mass 28. Because no signal at mass 42 is observed, we suggest the CO loss channel includes the following processes in dissociation:

(h)

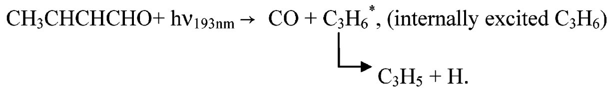

$$CH_3CHCHCHO + h\nu_{193nm} \rightarrow CO + C_3H_6^*, \text{(internally excited } C_3H_6) \qquad C_3H_6^* \rightarrow C_3H_5 + H.$$

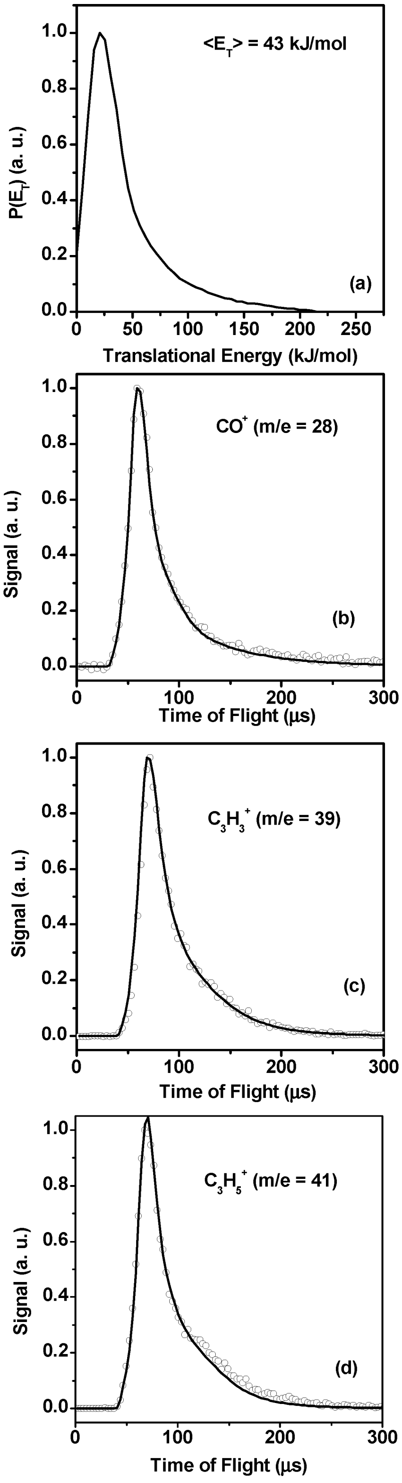

Figure 5. (a) CM translational energy distribution of CO elimination channel derived from the TOF spectra of CO^+ ($m/e = 28$). (b) TOF spectra of CO^+ ($m/e = 28$). (c) $C_3H_3^+$ ($m/e = 39$). (d) $C_3H_5^+$ ($m/e = 41$). All of them are collected at 10°. The 15, 12.2, and 9.3 eV photons are used as ionization sources for masses 28, 39, and 41, respectively. All of them are fitted with the $P(E_T)$ derived from TOF spectra of mass 28.

As mentioned above, the mass 29 loss channel only has a contribution to the TOF spectra of mass 41 when detected using ionization photons below 9.3 eV. Therefore, we assign the signal at mass 41, detected using higher photon energies to direct C_3H_5 formation, and the signal at mass 39 to the VUV dissociative photoionization product of C_3H_5. To fit the CO loss channel, we simplify the process by analyzing the data in two ways: first we ignore any possible contribution from other channels to the TOF spectra of mass 28; second we processed mass 41 as if it were the primary primary cofragment. We use this rationale because the CO loss channel is the dominant channel in the photofragmentation of crotonaldehyde.[16,17] In the secondary dissociation process $C_3H_6 \rightarrow C_3H_5 + H$, the H atom carries away most of translational energy released by the channel, thus the C_3H_5 fragment should have nearly the same translational energy as C_3H_6. The $P(E_T)$s derived from the TOF spectra of mass 28 are shown in Figure 5a. The maximum translational energy of the CO loss channel is ≈217 kJ/mol. The average kinetic energy of this channel is 43 kJ/mol. The TOF spectra of mass 28, 39, and 41, with their fits, are shown in Figure 5b−d.

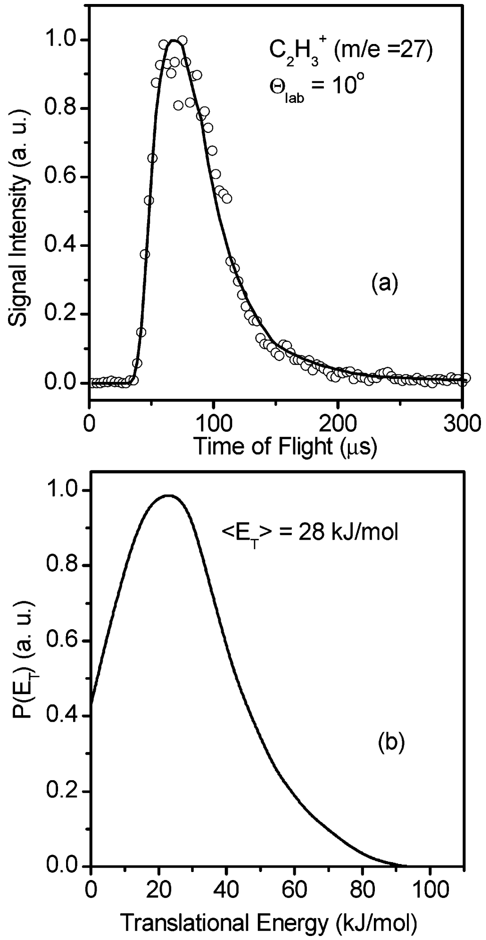

Figure 6. (a) TOF spectrum of mass 27 ($C_2H_3^+$) detected at 10° laboratory angle using 9.3 eV photons. (b) CM translational energy distribution of the $C_3H_6 \rightarrow CH_3 + CHCH_2$ secondary dissociation.

The signal at mass 27 ($C_2H_3^+$) observed in this experiment is assigned to another secondary dissociation product of C_3H_6*: $C_3H_6^* \rightarrow C_2H_3 + CH_3$. The structure of crotonaldehyde is such that the molecule ($CH_3CH{=}CHCHO$) has to isomerize before it can produce the primary product C_2H_3. In early studies of crotonaldehyde photolysis, McDowell suggested an isomerization in the process of crotonaldehyde photolysis: $CH_3CH{=}CHCHO + h\nu \rightarrow CH_2{=}CHCH_2CHO$.[7] This isomer could dissociate into $CH_2{=}CH$ and the CH_2CHO radical with a C−C bond rupture. However, our experimental results do not favor this idea, because we did not observe any signal at mass 43 (CH_2CHO^+) nor were we able fit the $P(E)$ derived from TOF spectra at masses 41, 40, and 39, the expected decomposition signatures for the CH_2CHO with the counterfragment of mass 27 (C_2H_3). Furthermore, the photon energy at 193 nm (618.9 kJ/mol) is not enough for $CH_2{=}CHCH_2CHO$ to undergo the direct three body dissociation: $CH_3CHCHCHO + h\nu_{193nm} \rightarrow C_2H_3 + CH_2 + HCO$ which requires 660 kJ/mol for this process to occur. The TOF mass spectrum with fitting is shown in the Figure 6a. The translational energy released during the secondary dissociation is shown in the Figure 6b. The average energy released in the secondary dissociation is 28 kJ/mol.

IV. Mechanism

Geometries and electronic properties are fundamental to understanding the photodissociation dynamics of molecules. However, there have been no theoretical calculations on the electronic configurations and energy levels of crotonaldehyde reported until very recently.[19,20] Walsh, using molecular orbital theory, derived the electron configuration of the ground and three lowest excited state of crotonaldehyde.[15] Referring to Walsh's studies and other studies on acrolein,[34,35] the configuration of the ground state and the lower excited states of the crotonaldehyde molecule may be represented as

$$\ldots (17a_1'')^2(18a_2'')^2\,(19a')^2,\ S_0,\ \text{the ground state}$$

$$\ldots (17a_1'')^2(18a_2'')^1\,(19a')^2(20a_2^*)^1,\ T_1(^3\pi\pi^*)$$

$$\ldots (17a_1'')^2(18a_2'')^2\,(19a')^1(20a_2^*)^1,\ T_2(^3n\pi^*)$$

$$\ldots (17a_1'')^2(18a_2'')^2\,(19a')^1(20a_2^*)^1,\ S_1\,(^1n\pi^*)$$

$$\ldots (17a_1'')^2(18a_2'')^1\,(19a')^2(20a_2^*)^1,\ S_2\,(^1\pi\pi^*)$$

The inner orbitals of crotonaldehyde molecule (not shown) are filled with the s electrons or σ electrons from the C−H, C−C, and C−O bonds. a_1'' and a_2'' represent the mixed π orbitals of the C=C and C=O bonds. a' stands for the nonbonding lone pair electrons of oxygen atom. a_2^* stands for the first antibonding π orbital. The conjugation between bonds in a molecule is a very interesting issue for organic chemists. Walsh was the first to suggest that for acrolein and crotonaldehyde, the two π orbitals of the C=C and C=O bonds are mixed, as are the two antibonding π orbitals of the C=C and C=O bonds. The a_1'' orbital lies below the normal π orbitals in energy, whereas the a_2'' lies above the normal π orbitals. The absorption spectra of acrolein and crotonaldehyde provide evidence of Walsh's suggestion. The $S_2 \leftarrow S_0$ transitions of the acrolein and crotonaldehyde molecules shift to much longer wavelengths compared with the similar transitions of ethylene and acetaldehyde.[15] Recently, studies done by Butler and co-workers give further evidence that the antibonding π orbital has a mixed π^*(C=C)/π^*(C=O) character for the excited state of acrolein, acrylic acid, and acryloyl chloride.[43] The conjugation between the two double bonds may not be complete. The a_1'' orbital may be localized more on the C=O bond than on the C=C bond, whereas the a_2'' orbital may be more localized on the C=C bond than on the C=O bond.[15] Compared with its isomer vinyl ketone, the conjugation interaction between these two double bonds combined with the inductive effect of the oxygen atom could result in a stronger molecular core for crotonaldehyde, which can make the heavy fragments of photodissociation survive. It is believed that the photodissociation of compounds with a C=C−C=O backbone usually pumps a large fraction of the available energy into the internal degrees of freedom of the fragments rather than into the fragments' translational motion.[43]

Of the four low lying excited states of the crotonaldehyde molecule, both the S_1 and the S_2 have been observed experimentally. The $S_1 \leftarrow S_0$ excitation requires at least 301 kJ/mol energy, and the $S_2 \leftarrow S_0$ excitation requires at least 477 kJ/mol energy.[15] The T_1 and T_2 states are 246 and 300 kJ/mol over the S_0, respectively.[19] Using 193.3 nm laser radiation, the excitation results in an $S_2 \leftarrow S_0$ transition for crotonaldehyde, a $\pi^* \leftarrow \pi$ electronic transition that is somewhat localized on the C=O double bond.

Among the three primary dissociation channels we observe, there are two dissociation channels, the H, and CH_3 loss channels, which result from a simple single step bond fission. The theoretical calculations on acrolein by Fang show that the mechanism of the H loss after 193 nm excitation is the following: the excited molecule first relaxes to the $^1n\pi^*$ state and then moves to the ground state via a curve crossing. The dissociation then proceeds on the ground-state surface forming two ground-state products. This is the most probable mechanism for the H loss channel of acrolein.[37] As we believe a similar process occurs in crotonaldehyde, both acrolein and crotonaldehyde may have very similar mechanisms for the H loss channel. The maximum translational energy of the CH_3 radical measured in this experiment is 113 kJ/mol. The available energy for the CH_3 loss channel is 210 kJ/mol (see Figure 1). These results imply that there is about 97 kJ/mol localized in internal excitation which could give rise to vibrationally excited products.

The CO loss channel is the only primary dissociation channel leading to a molecular loss channel in our experiment. Examining the mechanism of the CO loss channel of acrolein helps us to understand that of crotonaldehyde. Fang's theoretical studies on the photodissociation of acrolein show that the excited acrolein molecule (S_2) most probably relaxes to the T_1 state and then isomerizes to CH_3CHCO. The CH_3CHCO dissociation will proceed through the lowest triplet state to $CH_3CH + CO$. The CH_3CH immediately isomerizes to ground-state ethylene.[35] Fang suggested that the isomerization from CH_2CHCHO to CH_3CHCO might happen in the T_1 state, whose twisted equilibrium geometry induces a H-atom migration from the α carbon atom to the γ carbon atom. Experimental studies indicate the internal energy following the $CH_3CH + CO$ dissociation is distributed statistically.[26] CH_3CH has more vibrational modes than CO, so the CH_3CH fragment will carry most of the internal energy left in the fragments. Additionally, the isomerization reaction, $CH_3CH \rightarrow C_2H_4$ is exothermic by about 284 kJ/mol. Thus, the C_2H_4 fragment acquires most of the available energy in the CO loss channel. Lessard et al. reported the CO energy distributions from acrolein photodissociation at 193 nm. The average vibrational, rotational, translational energies of CO are about 17.1, 23.0, and 17.1 kJ/mol, respectively.[28] Compared with the available energy of the CO loss channel ($\approx$606 kJ/mol),[38] the CO fragment acquires only a small fraction of the available energy. These experimental results are consistent with the acrolein photodissociation mechanism put forward by Fang.

Crotonaldehyde has a similar structure to acrolein. Hence, the geometry-induced H atom migration from the α carbon atom to the γ carbon atom may also occur in the photodissociation of crotonaldehyde. This migration results in the isomerization of crotonaldehyde ($CH_3CHCHCHO$) to ethylketene (CH_3CH_2CHCO). We speculate that it is ethylketene that then decarbonylates. The unstable diradical CH_3CH_2CH immediately isomerizes into CH_3CHCH_2 (propene). This transformation will deposit significant internal energy in the nascent propene. The propene will then carry most of the available energy of the CO loss channel of crotonaldehyde (627 kJ/mol, see Figure 1). The hot propene decomposes spontaneously. The $CH_3CHCH_2 \rightarrow CH_2CHCH_2 + H$ and $CH_3CHCH_2 \rightarrow CH_3 + CHCH_2$ channels are observed in this experiment. The crucial step of decarbonylation of crotonaldehyde is an H-atom migration from the α carbon atom to the γ carbon atom, which results in the CO loss channel.

Initially, we believed mass 29 correlated to the HCO radical, its counterfragment being the CH_3CHCH radical. This was guided in part by earlier photodissociation work on acrolein where HCO was detected as a primary fragment. Very recently, Stolow and co-workers,[20] using femtosecond time-resolved photoelectron and coincidence spectroscopy, carried out photodissociation studies of a number of α,β enones. Interestingly, they found almost negligible amounts of HCO formation in their experiments with crotonaldehyde; acrolein photodissociation still produced HCO. Though the overall processes during relaxation are complicated, the results could be rationalized on the basis that the methyl group in crotonaldehyde hinders a torsional motion that promotes the $S_1 \rightarrow T_2$ intersystem crossing. This would diminish the HCO yield significantly, because it is via the T_2 state that dissociation to ground-state HCO takes place. They also speculate that there could be different decay dynamics in the case of crotonaldehyde, with triplet channels being not available for dissociation. Because their experimental technique was sensitive to only ground-state HCO, we thought it is possible that we were forming electronically excited-state HCO (energetically feasible in our experiment). However, it is well-known that the lowest electronically excited state, the $\tilde{A}(^2A'')$ state of HCO, predissociates rapidly due strong Renner−Teller interactions with the ground state[44] and the radical would not survive intact during the time it takes to reach the detector. This leaves only one another candidate for mass 29: C_2H_5 (ethyl radical). Although tunable synchrotron radiation is useful in separating out isomers and species with similar masses, in this case, unfortunately, we cannot distinguish these two radicals because their ionization energies are very nearly identical (8.117 eV (C_2H_5) vs 8.12 eV (HCO)). C_2H_5 could be formed by dissociation following the isomerization of crotonaldehyde to ethylketene, in a manner similar to that postulated for CO loss. Stolow and co-workers[20] also performed a time-resolved photoionization mass spectrometric study of the photodissociation of these enones. No mass 29 fragments were formed in the initial few picoseconds after photoexcitation, giving an apparent lower limit for the time scale of isomerization followed by fragmentation.

V. Conclusion

Analysis of the experimental results reveals that the photodissociation of crotonaldehyde at 193 nm proceeds along at least three dissociation channels: $CH_3CHCHCO + H$, $CH_3 + CHCHCHO$, and $CO + CH_3CHCH_2$. The enormous available energy of the $CO + C_3H_6$ channel causes the CH_3CHCH_2 fragment to undergo strong secondary dissociation. Referring to the photodissociation mechanism of acrolein, we suggest that the H atom loss channel of 193 nm photodissociation of crotonaldehyde proceeds along the ground-state potential energy surface and produces two ground-state products. The CO loss channel is facilitated by an H-atom migration from the α carbon atom to the γ carbon atom, and this migration is the isomerization of crotonaldehyde ($CH_3CHCHCHO$) into ethylketene (CH_3CH_2CHCO). The ethylketene dissociates into $CO + CH_3CHCH_2$, which is followed by strong secondary dissociation of hot CH_3CHCH_2.

Acknowledgment. This work is supported by the Director, Office of Science, Office of Basic Energy Sciences, Chemical Sciences Division of the US Department of Energy under contract No. DE-AC03-76SF00098. The Advanced Light Source is supported by the Director, Office of Science, Office of Basic Energy Sciences, Material Sciences Division of the U.S. Department of Energy under the same contract. J. Shu is grateful to Steve Harrich who generously permitted use of his excellent program for fitting the experimental data. We are indebted to Fei Qi and Paul Regan for providing insight into the dynamics of acrolein photodissociation.

References and Notes

(1) Graedel, T. E.; Hawkins, D. T.; Claxton, L. D. *Atmospheric Chemical Compounds: Sources, Occurrence and Bioassay*; Academic Press: Orlando, 1986.

(2) Orlando, J. J.; Tyndall, G. S.; Burkholder, J. B.; Bertman, S. B.; Chen, W. *Abstr. Pap. Am. Chem. Soc. 223*: 096-ENVR PART 1 APR 7 **2002**.

(3) Zervas, E.; Montagne, X.; Lahaye, J. *Environ. Sci. Technol*. **2002**, *36*, 2414−2421.

(4) Blacet, F. E.; Roof, J. G. *J. Am. Chem. Soc*., **1936**, *58*, 73−75.

(5) Volman, D. H.; Leighton, P. A.; Blacet, F. E.; Brinton, R. K. *J. Chem. Phys.* **1950**, *18*, 203−206.

(6) Harison, A. G.; Lossing, F. P. *Can. J. Chem.* **1959**, *37*, 1696−1702.

(7) McDowell, C. A.; Sifniades, S. *J. Am. Chem. Soc.* **1962**, *84*, 4606−4607.

(8) Grosjean, E.; Grosjean, D. *Int. J. Chem. Kinet.* **1998**, *30*, 21−29.

(9) Grosjean, E.; Grosjean, D. *J. Atmos. Chem*. **1997**, *27*, 271−289.

(10) Ullerstam, M.; Ljungström, E.; Langer, S. *Phys. Chem. Chem. Phys*. **2001**, *3*, 986−992.

(11) Thévenet, R.; Melllouki, A.; Bras, G. L. *Int. J. Chem. Kinet.* **2000**, *32*, 676−685.

(12) Albaladejo, J.; Ballesteros, B.; Jiménez, E.; Martín, P.; Martínez, E. *Atmos. Environ.* **2000**, *36*, 3231−3229.

(13) Cabañas, B.; Salgado, S.; Martín, P.; Baeza, M. T.; Martínez, E. *J. Phys. Chem. A* **2001**, *105*, 4440−4445.

(14) Stanton, B. J.; Monroe, E. T.; Wehry, E. L. *Anal. Chim. Acta* **1995**, *299*, 301−308.

(15) Walsh, A. D. *Trans. Faraday Soc.* **1945**, *41*, 498−505.

(16) Allen, E. R.; Pitts, J. N., Jr. *J. Am. Chem. Soc.* **1969**, *91*, 3135−3139.

(17) Coomber, J. W.; Pitts, J. N., Jr. *J. Am. Chem. Soc.* **1969**, *91*, 4955−4960.

(18) Magneron, I.; Thévenet, R.; Mellouki, A.; Bras, G. Le; Moortgat, G. K.; Wirtz, K. *J. Phys. Chem. A* **2002**, *106*, 2526−2537.

(19) Chen, I.-C. Reaction Channels of Crotonaldehyde, personal communication.

(20) Gessner, O.; Chrysostom, E. t-H.; Lee, A. M. D.; Wardlaw, D. M.; Ho, M.-L.; Lee, S.-J.; Cheng, B.-M.; Zgierski, M. Z.; Chen, I.-C.; Shaffer, J. P.; Hayden, C. C.; Stolow, A. *Faraday Discuss.* **2004**, *127*.

(21) Blacet, F. E.; Fielding, G. H.; Roof, J. G. *J. Am. Chem. Soc.* **1937**, *59*, 2375−2379.

(22) Coomber, J. W.; Pitts, J. N., Jr. *J. Am. Chem. Soc.* **1969**, *91*, 547−550.

(23) Gardner, E. P.; Sperry, P. D.; Calvert, J. G. *J Phys. Chem*. **1987**, *91*, 1922−1930.

(24) Jen, S. H.; Chen, I. C. *J. Chem. Phys*. **1999**, *111*, 8448−8453.

(25) Shinohara, H.; Nishi, N. *J. Chem. Phys*. **1982**, *77*, 234−245.

(26) Fujimoto, G. T.; Umstead, M. E.; Lin, M. C. *J. Chem. Phys*. **1985**, *82*, 3042−3044.

(27) Haas, B. M.; Minton, T. K.; Felder, P.; Huber, J. R. *J. Phys. Chem*. **1991**, *95*, 5149−5159.

(28) Lessard, P. C.; Rosenfeld, R. N. *J. Phys. Chem*. **1992**, *96*, 4615−4620.

(29) Parsons, F. B.; Szpunar, D. E.; Butler, L. J. *J. Chem. Phys*. **2002**, *117*, 7889−7895.

(30) Kao, Y. T.; Chen, W. C.; Yu, C. H.; Chen, I. C. *J. Chem. Phys*. **2001**, *114*, 8964−8970.

(31) Chowdhury, P. K.; Rao, K. V. S. R.; Mittal, J. P. *Chem. Phys. Lett*. **1994**, *218*, 60−66.

(32) Devaquet, A.; Salem, L. *Can. J. Chem*. **1971**, *49*, 977−979.

(33) Dykstra, C. E. *J. Am. Chem. Soc.* **1976**, *98*, 7182−7187.

(34) Lucchese, R. R.; Schaefer, H. F., III; Dykstra, C. E. *Chem. Phys. Lett.* **1977**, *51*, 600−602.

(35) Fridth, C.; Åsbrink, L.; Lindholm, E. *Phys. Scripta* **1979**, *20*, 603−304.

(36) Reguero, M.; Olivucci, M.; Bernardi, F.; Robb, M. A. *J. Am. Chem. Soc.* **1994**, *116*, 2103−2114.

(37) Fang, W. *J. Am. Chem. Soc*. **1999**, *121*, 8376−8384.

(38) Qi, F.; Regan, P. M.; Sorkhabi, O.; Suits, A. 193 nm Photodissociation of Acrolein Probed via VUV Synchrotron Radiation. Unpublished results.

(39) Lee, E. K. C.; Lewis, R. S. *Adv. Photochem*. **1980**, *12*, 1−95.

(40) Moore, C. B.; Weisshaar, J. C. *Annu. Rev. Phys. Chem.* **1983**, *34*, 525−555.

(41) Metha, G. F.; Terentis, A. C.; Kable, S. H. *J. Phys. Chem. A* **2002**, *106*, 5817−5827.

(42) Yang, X.; Lin, J.; Lee, Y. T.; Blank, D. A.; Suits, A. G.; Wodtke, A. M. *Rev. Sci. Instrum*. **1997**, *68*, 3317−3326.

(43) Arendt, M. F.; Browning, P. W.; Butler, L. J. *J. Chem. Phys.* **1995**, *103*, 5877−5885.

(44) Loison, J.-C.; Kable, S. H.; Houston, P. L. *Chem. Phys.* **1991**, *94*, 1796−1802.